Cement & Concrete Composites 34 (2012) 460–467

Contents lists available at SciVerse ScienceDirect

Cement & Concrete Composites

journal homepage: www.elsevier.com/locate/cemconcomp

Simulation of self-healing by further hydration in cementitious materials

Haoliang Huang [a,*], Guang Ye [a,b,1]

[a] Microlab, Faculty of Civil Engineering and Geosciences, Delft University of Technology, 2628CN Delft, The Netherlands
[b] Magnel Lab for Concrete Research, Department of Structural Engineering, Ghent University, Technologiepark-Zwijnaarde 904 B-9052, Ghent (Zwijnaarde), Belgium

ARTICLE INFO

Article history:
Received 14 June 2011
Received in revised form 27 December 2011
Accepted 3 January 2012
Available online 12 January 2012

Keywords:
Self-healing
Further hydration
Simulation
Thermodynamics model
Cementitious materials

ABSTRACT

Cracks, caused by shrinkage and external loading, facilitate the ingress of aggressive and harmful substances into concrete and indeed reduce the durability of the structures. It is well known that self-healing of cracks can significantly improve the durability of the concrete structure. In this research, self-healing of cracks was proposed to be realized by providing extra water for further hydration of unhydrated cement particles. In order to provide theoretical guidance for the practice, self-healing by providing extra water to promote further hydration was simulated. The simulation was based on water transport theory, ion diffusion theory and thermodynamics theory. In the simulation, self-healing efficiency under different conditions as a function of time was calculated. The relationship between self-healing efficiency and the amount of extra water from the broken capsules was determined. According to the results of the simulation, the amount of extra water can be optimized by considering self-healing efficiency and other performances.

1. Introduction

Cracks, caused by shrinkage and external loading, are unavoidable in reinforced concrete structures. These cracks facilitate the ingress of aggressive and harmful substances into concrete and indeed reduce the durability of the structures. Fortunately, cracks in concrete structures are able to heal under certain circumstance. For example, self-healing was directly observed in cracked water pipes and also found in some old structures [1,2]. Since self-healing of cracks can significantly prolong the service life of the concrete structures, it has attracted much attention in the last decade [3–8]. Some researchers investigated the mechanism of self-healing in water-filled cracks and concluded that further hydration of unhydrated cement and the nucleation of calcite were the main contributions of self-healing in cementitious materials [9–14]. As regards further hydration, in fact, a substantial amount of cement remains unhydrated over time due to the lack of water, especially in high performance concrete. If concrete cracks and extra water penetrates into the crack, further hydration of unhydrated cement will take place in the cracks. The formation and growth of hydration products will eventually heal the cracks.

In this research, the extra water is assumed to be stored in capsules which are pre-mixed in the cement paste. When the paste cracks, the cracks could pass through the capsules because of its low strength. In this way the water can be released from the capsules and induces further hydration of unhydrated cement particles. The cracks will be healed by the hydration products. Therefore, the self-healing process involves water transport, ion diffusion and precipitation of hydration products. The self-healing efficiency by further hydration is mainly determined by the width of the crack, the amount of unhydrated cement and available extra water. However, the quantitative relationships between these variables are not clear. In order to provide theoretical guidance for the practice, self-healing by providing extra water to promote further hydration was studied by numerical modeling.

According to the literature, microcracks are conventionally defined as the cracks whose widths are about a few micrometers (less than 10 μm) [15]. In this modeling, a microcrack, with the width of 10 μm, is supposed to propagate in the cement paste caused by shrinkage. Based on water transport theory in concrete, the amount of extra water in the crack was calculated as a function of time. Further hydration taking place in the water-filled crack was simulated with ion diffusion model and thermodynamics model. In order to simulate further hydration, the fraction and distribution of unhydrated cement particles were figured out by cement hydration and microstructural model HYMOSTRUC 3D [16–18]. With the HYMOSTRUC model, the hydration process of cement and the formation of microstructure can be simulated. Therefore, the fraction and distribution of unhydrated cement particles can be determined. The concentrations of ions dissolved from the unhydrated cement were calculated. When the concentrations of ions increase to a certain value, according to thermodynamic equilibrium, further hydration products start to precipitate. The amount of further hydration products was determined by thermodynamics model based on mass

* Corresponding author. Tel.: +31 15 2788343; fax: +31 15 2786383.
E-mail addresses: haoliang.huang@tudelft.nl (H. Huang), g.ye@tudelft.nl (G. Ye).
[1] Tel.: +31 15 2788343; fax: +31 15 2784001.

0958-9465/$ - see front matter © 2012 Elsevier Ltd. All rights reserved.
doi:10.1016/j.cemconcomp.2012.01.003

balance, charge balance and chemical equilibrium. In this way, self-healing efficiency as the function of time was determined. The relationship between the healing efficiency and amount of extra water is discussed as well.

2. Self-healing by further hydration

As shown in Fig. 1, it is assumed that the extra water is stored in capsules which are pre-mixed in the cement paste. When the paste cracks, the cracks can pass through the capsules, as well as some unhydrated cement particles. The unhydrated cement particles passed through by the crack are exposed on the crack surfaces, while the others are embedded inside the paste matrix.

2.1. Self-healing contributed by unhydrated cement on crack surfaces

The water stored in capsules is released immediately after the cement paste cracks and the cracks are filled with water. As shown in Fig. 1a, the unhydrated cement particles on the crack surfaces start to dissolve once they contact with water. Ca^{2+} ions begin to diffuse out from anhydrates immediately and then the silicate starts to diffuse out as well [19]. Consequently, the concentrations of various ions in the solution in the crack increase gradually. Once the concentrations of ions reach the equilibrium criteria for the precipitation, further hydration products are formed in the crack solution. During this further hydration processes, because there is plenty of CSH on the crack surfaces after the crack forms, induction period of hydration does not take place [20].

As further hydration products are formed at the unhydrated cement surfaces in the crack, further hydration gradually slows down and becomes more and more diffusion-controlled [16,21]. During this period, some parts of the ions are consumed to form the inner products while other parts of ions may diffuse into the crack solution. Therefore, the formation of healing products in the crack continues, but becomes slower and slower.

2.2. Self-healing contributed by unhydrated cement inside cement paste

In addition to the unhydrated cement on the crack surfaces, some ions also diffuse into the crack solution from the unhydrated cement embedded inside the cement paste, as shown in Fig. 1b. This diffusion can also increase the concentrations of ions in the solution in the crack, thus facilitates the formation of healing products in the crack. In this simulation, the contribution of the ions from the unhydrated cement particles inside the cement paste is also taken into account.

2.3. Effect of the absorption of cement paste on self-healing

In general, the concrete matrix is not fully saturated. Thus the concrete matrix is able to absorb water due to capillary action. Therefore, the water in cracks will be absorbed by the cement paste and the amount of water in the crack decreases. What should be mentioned is that the precipitation of further hydration products only takes place in the section of cracks which is entirely filled with water. When the water in the cracks is absorbed entirely, further hydration in cracks will stop.

3. Modeling system and computational methods

The simulation in this research is schematically shown in Fig. 2. A micro-crack with the size of 40 mm (length) × 40 mm (depth) × 10 μm (width) is supposed to pass through a capsule and also some unhydrated cement particles due to dense hydration products formed in the cement paste with low water to cement ratio. The surrounding surfaces of the cracked specimen are sealed and the crack is isolated with air. Therefore, the water in the crack cannot evaporate. Carbonation of calcite is prevented since no carbon dioxide can penetrate into the crack.

In the simulation, it is assumed that all the water stored in the capsules can be released into the cracks due to the capillary force. As mentioned, the water in the crack can be partly absorbed by the cement paste. The amount of water existing in the crack can be calculated with a water transport model, which is based on mass balance. Details are presented in Section 4.1.

Further hydration processes in the water-filled section of the cracks were simulated at the micro-level. A tiny square with the size of 100 μm × 100 μm (excluding the crack width) as simulation system from the water-filled section of crack is shown in Fig. 2. The distribution of unhydrated cement particles was simulated with HYMOSTRUC3D. The tiny square was discretized into micro-pixels with the size of 2 μm × 2 μm. The ion concentrations in each micro-pixel were calculated by the ion diffusion model based on Fick's second law. Meanwhile, a thermodynamics model based on chemistry equilibrium, mass balance and ion charge balance was utilized to simulate further hydration taking place in the micro-pixels. At each time step, the ion concentrations calculated by the diffusion model in each micro-pixel were input into the thermodynamics model. Through the thermodynamics model, the amount of further hydration products was calculated, as well as the ion concentrations after the chemical reaction. The outputs of concentration from the thermodynamics model were input into the diffusion model again as the initial conditions for the next step of the calculation. The condensed flowchart of the model for further hydration is shown in Fig. 3.

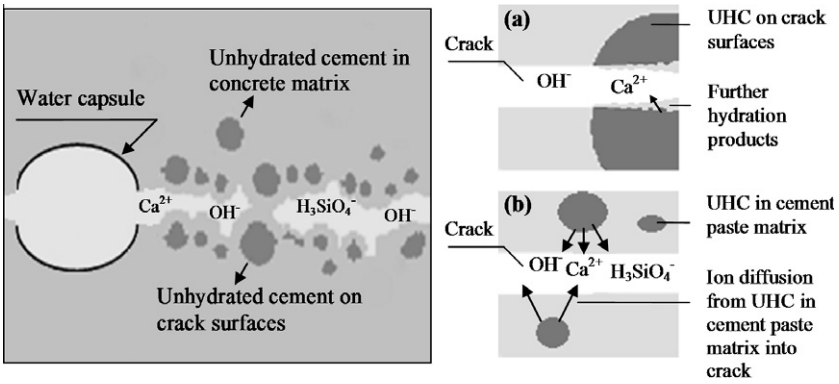

Fig. 1. Schematic diagram of the mechanism of further hydration: (a) further hydration of unhydrated cement on crack surfaces; (b) further hydration of unhydrated cement in cement matrix (UHC represents unhydrated cement particles).

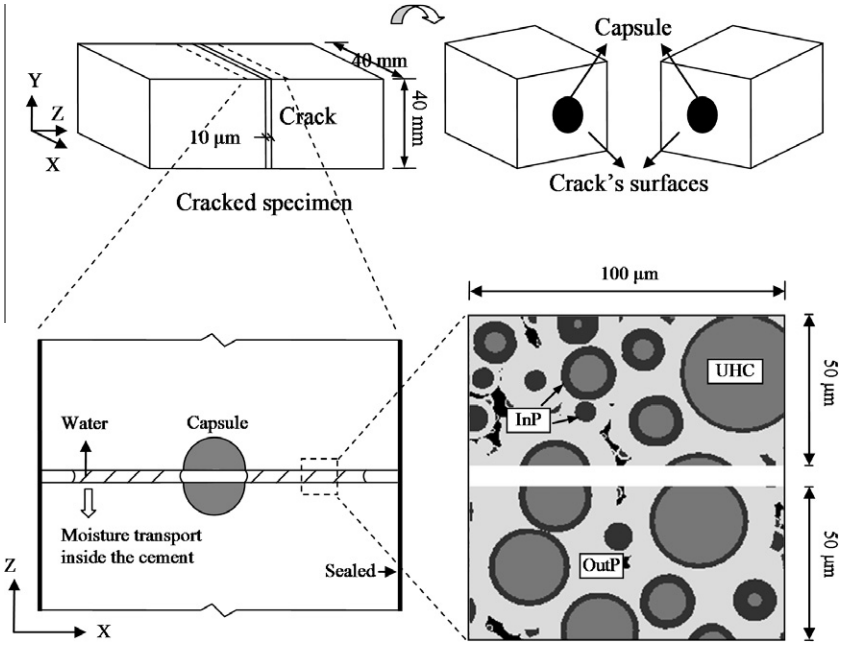

Fig. 2. Schematic diagram of modeling system (InP represents inner products, OutP represents out products, UHC represents unhydrated cement particles).

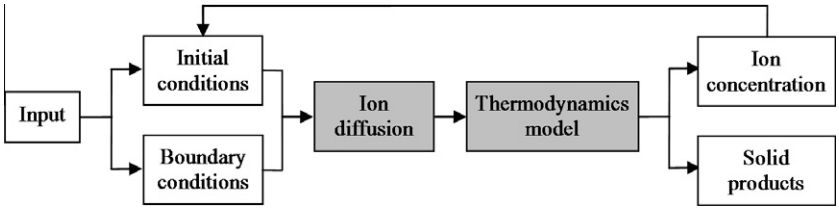

Fig. 3. Flowchart of the model for further hydration.

The self-healing efficiency, defined as the volume ratio of newly formed hydration products to the volume of the crack, can be determined by coupling the water transport and further hydration of cement particles. Detailed information about the coupling is presented in Section 6.2.

4. Theory

4.1. Water transport from cracks into the matrix

In general, the pore space of cement paste is not fully saturated. Water will therefore penetrate into the cement paste once the cracks are filled with water. According to the mass balance, the decrease of water volume in the crack should be equal to the increase of water volume in the cement paste, which is expressed as:

$$\Delta V_{con} = -\Delta V_{cra} \tag{1}$$

where ΔV_{cra} (m^3) is the water volume in the crack, ΔV_{con} (m^3) is the water volume in the cement paste.

The relationship between the water volume in cement paste and the degree of saturation can be expressed as:

$$\Delta V_{con} = \sum_i \Delta s_i \cdot \phi \cdot V_i \tag{2}$$

where V_i (m^3) is the volume of cement paste in ith element, Δs_i (–) is the variation of the degree of saturation, and ϕ (–) is the porosity.

Therefore, the volume of water in cracks as the function of time can be calculated as:

$$V_{cra}(t) = V_{cra,o} - \sum_i \Delta s_i(t) \cdot \phi \cdot V_i \tag{3}$$

where $V_{cra,o}$ (m^3) is the total volume of available extra water.

The variation of the degree of saturation in cement paste can be described by the extensive Darcy's law [22]:

$$\frac{\partial s}{\partial t} = \nabla \cdot \left[(k_l + k_v) \frac{\partial p}{\partial s} \nabla s \right] \tag{4}$$

where k_l (1/(N s)) is the unsaturated permeability depending on the degree of saturation, k_v (1/(N s)) is the vapor diffusion coefficient in pores. In this study, the vapor diffusion is minor and neglected. k_l can be calculated as [23]:

$$k_l = \frac{\rho \phi^2}{50 B^2 \mu} \cdot \left[1 - \ln\left(\frac{e}{1-s}\right) \cdot (1-s) \right]^2 \tag{5}$$

where ρ (kg/m^3) is the water's density; ϕ is the porosity of the cement paste; B (1/m) is constant of Reyleigh-Ritz pore size distribution, which represents the peak of pore size distribution on a logarithmic scale; μ (Pa s) is the viscosity of water under ideal conditions of the connected pores; $e \approx 2.72$, which is mathematical constant.

The relationship between the capillary force and degree of saturation can be expressed as [23]:

$$\frac{\partial p}{\partial s} = \frac{2BC\gamma \cos\alpha}{(1-s)\ln^2(1-s)} \tag{6}$$

where C (–) is the constant, which is determined as 2.15 according to the literature [23]; γ (N/m) is surface tension of water; α (°) is contact angle between water and solid.

According to Eqs. (3)–(6), the volume of water in cracks as the function of time can be calculated.

4.2. Further hydration

As mentioned above, further hydration process includes ion diffusion and precipitation of further hydration products. The theories used to describe these two phenomenons are presented in the following.

4.2.1. Ion diffusion

In this simulation, ion diffusion takes place both in crack space and cement paste matrix. The ion diffusion in both systems can be described by Fick's second law [24]:

$$\frac{\partial c_i}{\partial t} = \nabla \cdot (D_i \nabla c_i) \tag{7}$$

where c_i (mol/m^3) is the concentration of the ith ion and D_i (m^2/s) is the diffusion coefficient of the ith ion.

Inside the crack, when hydration products are formed, the ion diffusion from the cement paste matrix to the crack is hampered. Therefore, the diffusion coefficient in the water-filled cracks decreases with the increase of further hydration products. In the model, the diffusion coefficient in the water-filled cracks is calculated as:

$$D_i = D_{i,0} - (D_{i,0} - D_{i,HP}) \cdot \varphi \tag{8}$$

where $D_{i,0}$ (m^2/s) is the initial diffusion coefficient in solution without solid phases; $D_{i,HP}$ (m^2/s) is the diffusion coefficient in hydration products. φ (–) is the fraction of solid phases in the pixel-elements of water-filled cracks. For the diffusion inside the hydration products in the cement paste matrix, the diffusion coefficient is $D_{i,HP}$ (m^2/s).

As shown in Fig. 2, the crack surfaces are composed of unhydrated cement and hydration products which are formed before the crack appears. Based on this, the boundary conditions of ion diffusion inside the crack are classified as boundary conditions for unhydrated cement and hydration products. The amount of ions dissolved from the unhydrated cement is related to the penetration depth of the unhydrated cement particle. The mathematical expression of the boundary conditions for unhydrated cement particle surface is written as:

$$\frac{\partial c_{i,S-UHC}}{\partial n} = -\frac{d\theta(\delta)}{D_{i,s} \cdot \Delta A_{UHC} \cdot dt} \tag{9}$$

where $c_{i,S\text{-}UHC}$ (mol/m^3) is the concentration of the ith ion on the surface of unhydrated cement; n is the normal direction of the crack surface; A_{UHC} (m^2) is the area of the unhydrated cement particle contacting with crack solution; t (s) is diffusion time; $D_{i,s}$ (m^2/s) is diffusion coefficient of the ith ion on the unhydrated cement particle surfaces; $\theta(\delta)$ (mol) is the number of mol of the ith ion diffusing from the unhydrated cement as the function of penetration depth δ (m). The penetration depth δ is the depth of hydration products which occupy the original space of unhydrated cement.

According to Section 2, the unhydrated cement particles are discretized into micro-pixels. The hydration can be simplified as flat surface reaction of the pixels which represent the surfaces of unhydrated cement particles. The rate of phase-boundary reaction can be described as [16]:

$$\frac{d\delta}{dt} = R \tag{10}$$

where R depends on the chemical composition of the reactant and the ion concentration in the liquid phase. For the diffusion-controlled reactions, the reaction rate can be expressed as:

$$\frac{d\delta}{dt} = \frac{R}{\delta} \tag{11}$$

In addition to the boundary of unhydrated cement (described by Eq. (9)), the boundary of hydration products (formed before crack appears) on the crack surface can be described by Robin boundary conditions (the third type boundary conditions) [25]:

$$\frac{\partial c_{i,S\text{-}CP}}{\partial n} + \frac{\sigma}{D_{i,0}} \cdot c_{i,S\text{-}CP} = \frac{\sigma}{D_{i,0}} \cdot c_{i,CP} \tag{12}$$

where $c_{i,S\text{-}CP}$ (mol/m^3) is the concentration of the ith ion on the surface of cement paste on crack surfaces; n is the normal direction of the crack surface; $D_{i,0}$ (m^2/s) is diffusion coefficient of the ith ion in the solution of the crack; σ is the exchange coefficient between the solution in the crack and the hydration products on the crack surfaces. According to the reference [25], σ can be calculated by the formula:

$$\sigma = d\theta / [(c_{i,CS} - c_{i,CP}) \cdot \Delta A_{HP} \cdot dt] \tag{13}$$

where $c_{i,CS}$ (mol/m^3) is the concentration of the ith ion in the crack solution near the crack surfaces; $c_{i,CS}$ (mol/m^3) is the concentration of the ith ion in the pore of the cement paste near the crack surfaces; A_{HP} (m^2) is the area of the hydration products (formed before the crack appears) on crack surfaces; $d\theta$ (mol) is the number of mol of the ith ion diffusing from the hydration products (on the crack surface) into the crack solution. Because the amounts of ions diffusing through the CSH and CH are very limited [26], it is assumed that the ion diffusion in the hydration products is mainly through the capillary pores. Therefore, $d\theta$ can be calculated by the formula:

$$d\theta = -D_{i,0} \cdot \Delta A_{HC} \cdot \phi \cdot dt \cdot (c_{i,CS} - c_{i,CP})/L \tag{14}$$

where L is the length of each pixel, which is 2 μm in this study.

For the ion diffusion inside the cement paste matrix, the boundary conditions for the surface of unhydrated cement particles embedded in the paste can be also expressed by Eq. (9). What should be mentioned is that the penetration depth of the cement particles inside the cement paste should be calculated according to the age of the cement paste, rather than the saturation time of the crack. Regarding the boundary with the crack solution, it can be described by Robin boundary conditions as well.

4.2.2. Thermodynamics model for further hydration

Accompanying with the dissolution of the clinkers and the ion diffusion, the precipitation of solids in the crack solution can be described by the thermodynamics model. This model was established based on the assumption of thermodynamics equilibrium, mass balance and charge balance. The mathematic description of the model is presented as the governing equations.

The cement–water system containing N chemical species was considered. In this system, there are l independent chemical reactions taking place. The charge balance for the ions involved in hydration process in the system can be written as [27]:

$$\sum_{i=1}^{N} Z_i c_i \tag{15}$$

where i is the number of the species and Z_i (–) is the valence (including sign) of the ith species. For example, Z_i would be −2 for $SiO_2(OH)_2^{2-}$.

In this reaction system, the mass of each chemical element before and after chemical reaction should keep balance, which is given as [27]:

$$B_e - \sum_e b_e c_e = 0 \tag{16}$$

where B_e (mol/m^3) is the molar concentration of the element e in the system (such as $\sum$Ca in this modeling) and b_e (–) is the number

Table 1
Details of paste matrix.

Main compositions of cement (wt.%)				Water/cement ratio	Age (h)
C_3S	C_2S	C_3A	C_4AF		
65.8	14.8	8.3	11.1	0.3	1000

Table 2
Parameters for water transport model.

Porosity	Initial degree of saturation s_0	Viscosity of water μ (Pa s)	Surface tension γ (N/m)	Constant B (1/m)	Constant C
0.08	0.78	0.001	0.0728	3.6×10^7	2.15

of the atoms of the element e in the chemical formula of every species. For example, in this modeling the mass balance equation for the element Ca, b_e for the species $(Ca(OH)_2)_2(SiO_2)_{2.4}\cdot(H_2O)_2$ should be 2.

The equilibrium equations can be expressed as [27]:

$$-\log K_k + \sum_{i=1}^{N} v_{ki} \log \beta_i + \sum_{i=1}^{N} v_{ki} \log c_i = 0 \tag{17}$$

where K_k is the equilibrium constant for the kth chemical reaction (in this simulation, there are five reactions for further hydration. It means that $k = 5$); v_{ki} is the number of times the ith species occurring in the kth chemical reaction; β_i is the activity coefficient of the ith species. The set of Eqs. (15)–(17) constitute a nonlinear system which can be dissolved by Newton–Raphson method. Eqs. ((15)–(17)) can be generalized as:

$$\Psi(c_i) = 0 \tag{18}$$

According to Newton–Raphson method, the Eq. (18) can be approximated by the linear system as follow [28]:

$$c_{i,n+1} = c_{i,n} - \Psi(c_{i,n})/\Psi'(c_{i,n}) \tag{19}$$

Eq. (19) can be rewritten as:

$$\Psi'(c_{i,n}) \cdot \delta c_i = -\Psi(c_{i,n}), \quad c_{i,n+1} = \delta c_i + c_{i,n} \tag{20}$$

The concentration of ith species can be calculated when the iteration is the convergent according to Eq. (20).

5. Modeling parameters

5.1. Materials

In the simulation, the details of the cement paste matrix are shown in Table 1.

5.2. Parameters for water transport model

In the simulation, the water to cement ratio of the matrix is 0.3 and the age of the paste is 1000 h. According to the simulation by HYMOSTRUC3D, the degree of hydration is 0.7 and the porosity is 0.08. The relative humidity is about 75% when the degree of hydration is 0.7 [16]. According to Power's model, the initial degree of saturation approximates 0.78 [29]. The parameters used in the simulation of water transport from cracks into the cement paste matrix are shown in Table 2.

5.3. Parameters for further hydration model

5.3.1. Kinetics of cement hydration

As mentioned, the unhydrated cement particles are represented by micro-pixels in the model. The hydration can be simplified as flat surface reaction of the pixels which represent the unhydrated cement particles. The rate of reaction is described by Eqs. (10) and (11). In the model, the parameter R related to the rate of reaction is cited as [16]: $R = 0.045$ μm/h.

5.3.2. Fraction and distribution of unhydrated cement

In order to simulate further hydration in the crack, the fraction and distribution of unhydrated cement particles were simulated by HYMOSTRUC3D, as shown in Fig. 4. After hydration for 1000 h, there is around 30% of the cement remains unhydrated in the matrix.

5.3.3. Chemical reaction and species

In the simulation, only the further hydration of C_3S and C_2S was considered in the self-healing process. The chemical reactions and equilibrium constants involved in further hydration are presented in Table 3. The species in the solution are shown in Table 4.

6. Results and discussion

6.1. Water transport from cracks into matrix

After the capsules are broken by the crack, the extra water is released into the crack immediately. It should be mentioned that the

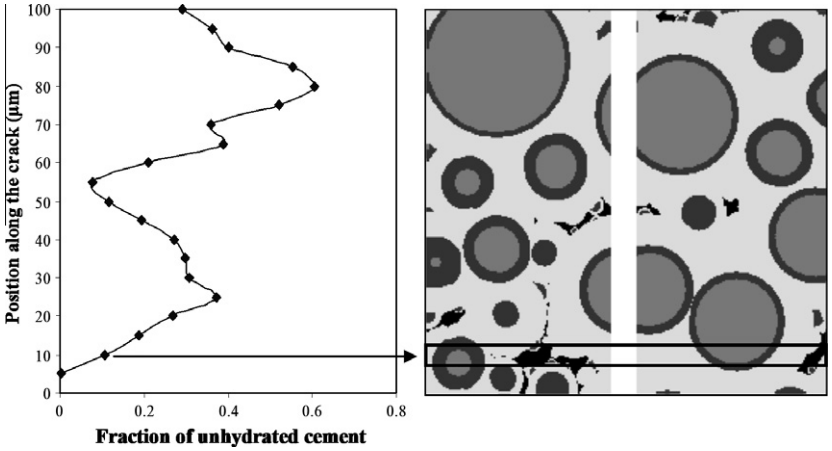

Fig. 4. Fraction and distribution of unhydrated cement.

Table 3
Chemical reactions in the modeling.

Chemical reaction	log k	Reference
$CaOH^+ \Longleftrightarrow Ca^{2+} + OH^-$	−1.18	Hummel et al. [30]
$H_2O \Longleftrightarrow OH^- + H^+$	−14.00	Hummel et al. [30]
$H_3SiO_4^- \Longleftrightarrow H_2SiO_4^{2-} + H^+$	−13.33	Hummel et al. [30]
$CaH_2SiO_4 \Longleftrightarrow Ca^{2+} + H_2SiO_4^{2-}$	−8.6	Mazibur Rahman et al. [31]
$Ca(OH)_2 \Longleftrightarrow Ca^{2+} + 2OH^-$	−5.19	Reardon [32]

Table 4
Chemical species in the modeling.

No.	1	2	3	4	5	6	7	8	9
Species	Ca^{2+}	OH^-	H^+	H_2O	$H_3SiO_4^-$	$CaOH^+$	$H_2SiO_4^{2-}$	$Ca(OH)_2$	CaH_2SiO_4

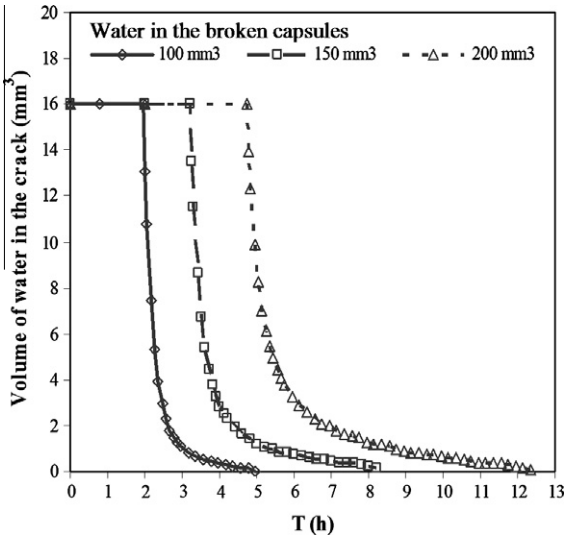

Fig. 5. Amount of water in the crack at different time.

amount of water released into cracks is less than the amount of capsules because only some fraction of capsules are passed through by the cracks. Regardless of the shape and size of the capsules, only the amount of water which is able to be released was taken into account in the model.

Fig. 5 shows the amount of water in the crack at different time. For the crack with the size of 40 mm (length) × 40 mm (depth) × 10 μm (width), the volume of crack space is 16 mm^3. Some extra water is still stored in the broken capsules if the total volume of extra water in broken capsules is larger than 16 mm^3. The whole crack keeps saturated until the extra water stored in broken capsules is used up. When there is no more water provided from the broken capsules, the volume of water in the crack stars to decrease with the transport into the matrix. As shown in Fig. 5, after the capsules which store 100 mm^3 of water are broken by the crack, the amount of water in the crack is equal to the crack space (16 mm^3) until 2 h. It means that the whole crack keeps saturated for 2 h. In comparison, the volume of water in the crack keeps as much as 16 mm^3 until 3.2 h when there is 150 mm^3 water stored in the broken capsules. In the case of 200 mm^3 of extra water, the time for the crack keeping saturated increases to 4.7 h. As mentioned above, self-healing only takes place in the water-filled section of the crack. Therefore, self-healing in the whole crack is simulated until the extra water stored in broken capsules is used up. After the extra water in broken capsules is used up, the water-filled section of the crack decreases. Further hydration

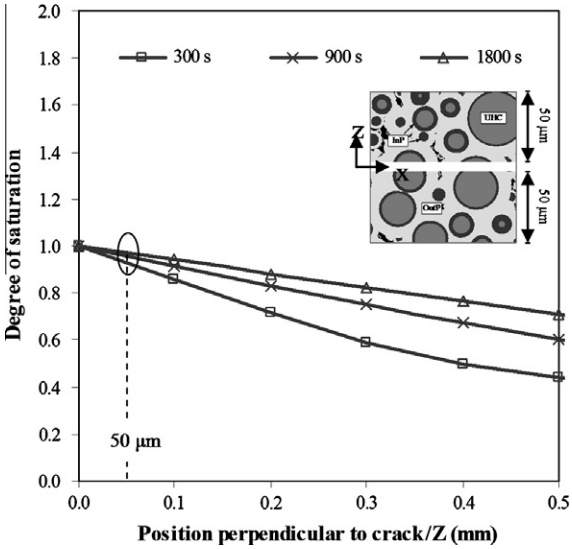

Fig. 6. Degree of saturation of the matrix close to the crack.

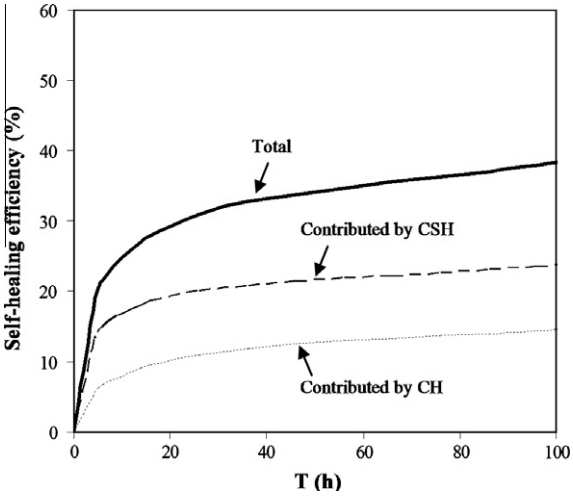

Fig. 7. Self-healing efficiency of crack under saturation condition.

stops in the section of crack without water and the modeling system in micro-level for this section will be "locked" and no more healing products will be formed.

Fig. 6 shows the water content of the cement paste perpendicular to the crack. As the water penetrates into the matrix from the crack, the water content in cement paste increases. After the water is released into the crack for 300 s, the degree of saturation in the cement paste at the distance of 50 μm from the crack surface is about 0.93. This value increases to 0.99 when the time is 1800 s. Therefore, in the simulation the ion diffusion from unhydrated cement particles into the water-filled crack was assumed to take place under saturation condition.

6.2. Self-healing of cracks by further hydration

6.2.1. Self-healing of cracks under saturation condition

Fig. 7 shows self-healing efficiency by further hydration under saturation condition. Since some unhydrated cement particles are passed by the crack and exposed on the crack inside surfaces, further hydration takes place immediately after these cement particles contact with water. The amount of hydration products in the crack increases dramatically during the first 20 h. After

Table 5
Calculation of healing efficiency by coupling saturation and nonsaturation condition.

Condition	Time (h)	Volume of extra water in cracks/v_i (mm^3)	Healing efficiency under saturation condition/$p_{s,i}$ (%)	Healing efficiency by coupling nonsaturation/$p_{us,i}$ (%)
Saturation	0.0	16.0	0.00	0.00
	0.1	16.0	0.42	0.42
	⋮	⋮	⋮	⋮
	2.0	16.0	8.26	8.26
Nonsaturation	2.1	10.8	8.68	8.58
	2.2	7.5	9.10	8.77
	2.3	5.3	9.52	8.91
	2.4	3.9	9.94	9.01
	2.5	2.9	10.36	9.09
	2.6	2.3	10.78	9.15
	⋮	⋮	⋮	⋮
	4.8	0.1	19.74	9.48
	4.9	0	20.28	9.48

20 h, the speed of self-healing of the crack starts to slow down. The reason is that the transport of ions to and from the surface of the unhydrated cement particle is getting more and more difficult as further hydration products are formed around the unhydrated cement. From the modeling results, it can be learned that after 20 h of further hydration about 30% of the crack's volume is healed when the width of crack is 10 μm under saturation condition.

6.2.2. Self-healing of cracks under condition from saturation to nonsaturation

In the real situations, the saturation of the crack changes with the transport of water in cement paste. The self-healing efficiency should be calculated by coupling the results of water transport (Fig. 5) and the healing efficiency under saturation condition (Fig. 7). The calculation is shown in Table 5.The formula for the calculation can be written as:

$$p_{us,i} = \begin{cases} p_{s,i}, v_i = v_c \\ p_{us,i-1} + v_i \cdot (p_{s,i} - p_{s,i-1})/v_c, \quad v_i \leqslant v_c \end{cases} \tag{21}$$

where $p_{us,i}$ is the self-healing efficiency for which nonsaturation condition are also taken into account; v_c is the volume of cracks, in this simulation $v_c = 16\ mm^3$; v_i is the volume of water in the crack, which is shown in Fig. 5; $p_{s,i}$ is the healing efficiency under saturation condition, which is shown in Fig. 7.

The self-healing efficiency for which nonsaturation condition are also taken into account is presented in Fig. 8. When 100 mm^3 of water is provided into the crack, of which the size is 40 mm (length) × 40 mm (depth) × 10 μm (width), self-healing efficiency rises sharply in the first 2 h. After 2 h, the water provided by broken capsules becomes less and less, thus the increasing rate of self-healing efficiency gets smaller and smaller. After all the water in the crack was consumed, self-healing efficiency becomes steady. While 150 mm^3 of water is provided, the crack is able to keep saturated for more than 3 h. Therefore, self-healing efficiency is much higher than that of 100 mm^3 of extra water. When 200 mm^3 of extra water is available, self-healing efficiency increases apparently until 4.7 h. After that, it almost reaches the maximum value.

6.2.3. Self-healing efficiency and the amount of extra water from broken capsules

The relationship between the final self-healing efficiency and the amount of extra water released from broken capsules is shown in Fig. 9. The final self-healing efficiency rises with the increase of extra water at two different rates. When 100 mm^3 of water is provided into the crack, of which the size is 40 mm (length) × 40 mm (depth) × 10 μm (width), the final self-healing efficiency is about 9.5%. While the broken capsules provide 150 mm^3 of water, the final self-healing efficiency increases to 15.3%. With this significant rate, the final self-healing efficiency rises to 22.9% when the extra water increases to 250 mm^3. However, the increasing rate of healing efficiency slows down after this point. This relationship between self-healing efficiency and the amount of water can be analyzed by coupling Figs. 5 and 7. Further hydration products increase dramatically before 7 h. This is the reason why the increasing rate of self-healing efficiency is large when the amount of extra water increases from 100 mm^3 to 250 mm^3. However, as shown in Fig. 7, the formation of further hydration products starts to slow down gradually after 7 h. Therefore, the increasing rate of healing efficiency to the amount of extra water slows down when the water is more than 250 mm^3.

What should be mentioned is that as shown in Table 3, in the simulation the CSH gel was assumed as CaH_2SiO_4, which contains absolutely only 1 unit of chemically bound water per mole and no gel water was taken into account. From the literatures, however, the water content of CSH gel in cement paste is higher than this value, for example, the jennite ($Ca_{1.5}Si_{0.9}O_{1.8}(OH)_3{\cdot}0.9H_2O$)

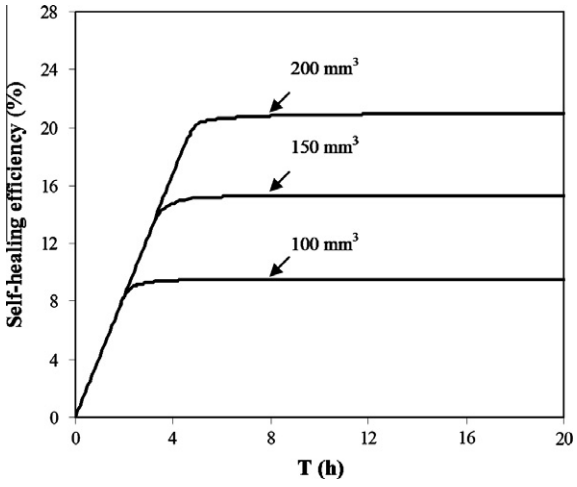

Fig. 8. Self-healing efficiency at different time by providing extra water.

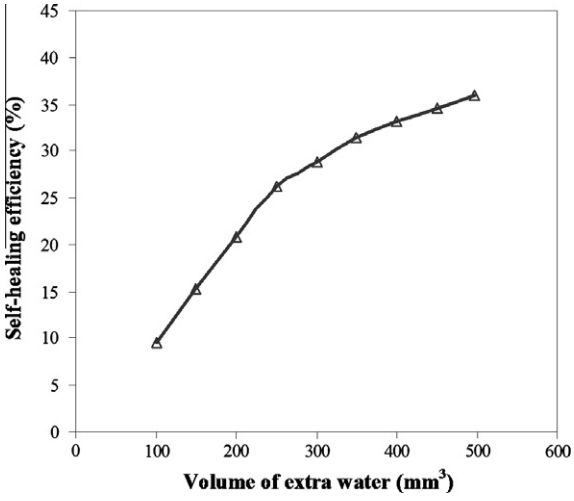

Fig. 9. Self-healing efficiency by providing different amount of extra water.

[33,34]. Therefore, in this simulation the consumption of water in the self-healing process is slightly underestimated. However, as discussed in Section 6.1, the decrease of water in the crack is mainly caused by the capillary absorption of the cement paste. Therefore, the effect caused by the underestimation of the consumption of water for the formation of CSH is slight.

Based on the simulation, the quantitative relationships between self-healing efficiency, the amount of unhydrated cement and the extra water provided were determined. In practice, in order to consider other performances of the concrete, such as the strength, it is impossible to add too many capsules into the concrete matrix. With the results of this simulation, the optimized amount of extra water can be determined by considering self-healing efficiency and other performances. Further research about this will be carried out in the future.

7. Conclusions

Self-healing by providing extra water to promote further hydration was simulated in this paper. Based on water transport theory, the volume of extra water in the crack was calculated as the function of time. Further hydration taking place in the water-filled crack was simulated with ion diffusion model and thermodynamics model. In order to simulate further hydration, the fraction and distribution of unhydrated cement particles were simulated by HYMOSTRUC3D. The concentrations of ions dissolved from the unhydrated cement were calculated. When the concentrations of ions increase to a certain value, further hydration products start to precipitate. The amount of further hydration products was determined by thermodynamics model based on mass balance, charge balance and chemical equilibrium. Through the simulation of self-healing by further hydration, the relationship between self-healing efficiency and the amount of extra water released from broken capsules was quantified. According to the results of the simulation, the amount of extra water can be optimized by considering self-healing efficiency and other performances.

Acknowledgements

The authors would like to thank the China Scholarship Council (CSC) for the financial support for this work. All reviews' constructive comments and suggestions are gratefully appreciated.

References

[1] Turner L. The autogenous healing of cement and concrete: its relation to vibrated concrete and cracked concrete. In: Proceedings of international association for testing materials. London; 1937.
[2] Nijland TG, Larbi JA, van Hees RPJ, Lubelli B, de Rooij MR. Self-healing phenomena in concretes and masonry mortars: a microscopic study. In: van der Zwaag S, editor, 1st international conference on self-healing materials. Dordrecht; 2007.
[3] Dry C. Three-part methylmethacrylate adhesive system as an internal delivery system for smart responsive concrete. Smart Mater Struct 1996;5(3):297–300.
[4] Li VC, Lim YM, Chan Y-W. Feasibility study of a passive smart self-healing cementitious composite. Compos Part B: Eng 1998;29(6):819–27.
[5] Van Tittelboom K, De Belie N, Van Loo D, Jacobs P. Self-healing efficiency of cementitious materials containing tubular capsules filled with healing agent. Cem Concr Compos 2011;33(4):497–505.
[6] Yang Z, Hollar J, He X, Shi X. A self-healing cementitious composite using oil core/silica gel shell microcapsules. Cem Concr Compos 2011;33(4):506–12.
[7] Granger S, Loukili A, Pijaudier-Cabot G, Chanvillard G. Experimental characterization of the self-healing of cracks in an ultra high performance cementitious material: mechanical tests and acoustic emission analysis. Cem Concr Res 2007;37(4):519–27.
[8] Granger S, Pijaudier Cabot G, Loukili A, Marlot D, Lenain JC. Monitoring of cracking and healing in an ultra high performance cementitious material using the time reversal technique. Cem Concr Res 2009;39(4):296–302.
[9] Evardsen C. Water permeability and autogenous healing of cracks in concrete. ACI Mater J 1999;96(4):448–54.
[10] Ahn TH, Kish T. Crack self-healing behavior of cementitious composites incorporating various mineral admixtures. J Adv Concr Technol 2010;8(2):16.
[11] Qian S, Zhou J, de Rooij MR, Schlangen E, Ye G, van Breugel K. Self-healing behavior of strain hardening cementitious composites incorporating local waste materials. Cem Concr Compos 2009;31(9):613–21.
[12] Kan Li-Li, Shi H-S, Sakulich Aaron R, Li Victor C. Self-healing characterization of engineered cementitious composite materials. ACI Mater J 2010;107(6):8.
[13] He H, Guo Z, Stroeven P, Stroeven M, Sluys LJ. Self-healing capacity of concrete – computer simulation study of unhydrated cement structure. Image Anal Stereol 2007;26:137–43.
[14] Schlangen E, ter Heide N, van Breugel K. Crack healing of early age cracks in concrete. In: Konsta-Gdoutos MS, editor. Measuring, monitoring and modeling concrete properties. Netherlands: Springer; 2006.
[15] Ammouche A, Riss J, Breysse D, Marchand J. Image analysis for the automated study of microcracks in concrete. Cem Concr Compos 2004;23(2–3):267–78.
[16] van Breugel K. Simulation of hydration and hormation of structure in hardening cement-based materials. Thesis (PhD). Delft University of Technology; 1991.
[17] Koenders EAB. Simulation of volume changes in hardening cement-based materials. Thesis (PhD). Delft University of Technology; 1997.
[18] Ye G. Experimental study and numerical simulation of the development of the microstructure and permeability of cementitious materious. Thesis (PhD). Delft University of Technology; 2003.
[19] Dent Glasser LS, Lachowski EE, Mohan K, Taylor HFW. A multi-method study of c3s hydration. Cem Concr Res 1978;8(6):733–9.
[20] Odler I, Dorr H. Early hydration of tricalcium silicate ii. The induction period. Cem Concr Res 1979;9(3):277–84.
[21] Taylor HFW. Cement chemistry. London: Thomas Telford Publishing; 1997.
[22] Cerny R, Rovnanikova P. Transport process in concrete. London: Taylor & Francis; 2002.
[23] Maekawa K, Chaube R, Kishi T. Modeling of concrete performance: hydration, microstructure and mass transport. London: E & FN Spon.; 1999.
[24] Cussler EL. Diffusion: mass transfer in fluid systems. UK: Cambridge university press; 1997.
[25] Crank J. The mathematics of diffusion. Oxford: Clarendon Press; 1956.
[26] Garboczi EJ, Bentz DP. Computer simulation of the diffusivity of cement-based materials. J Mater Sci 1992;27(8):2083–92.
[27] Anderson GM, Crerar DA. Thermodynamics in geochemistry: the equilibrium model. New York: Oxford University Press; 1993.
[28] Press WH, Flannery BP, Teukolsky SA, Vetterling WT. Numerical recipes in fortran. Cambridge: Cambridge University Press; 1992.
[29] Powers TC, Brownyard TL. Studies of the physical properties of hardened portland cement paste (9 parts). J Am Concr Inst 43, Bulletin 22, Chicago; 1948.
[30] Hummel W, Berner U, Curti E, Thoenen T. Nagra/psi chemical thermodynamic data base 01/01. USA: Universal Publishers; 2002.
[31] Mazibur Rahman Md, Nagasaki S, Tanaka S. A model for dissolution of CaO–SiO_2–H_2O gel at Ca/Si > 1. Cem Concr Res 1999;29(7):1091–7.
[32] Reardon EJ. An ion interaction model for the determination of chemical equilibria in cement/water systems. Cem Concr Res 1990;20(2):175–92.
[33] Lothenbach B, Winnefeld F. Thermodynamic modelling of the hydration of portland cement. Cem Concr Res 2006;36(2):209–26.
[34] Lothenbach B. Thermodynamic equilibrium calculations in cementitious systems. Mater Struct 2010;43(10):1413–33.